Journal of the European Ceramic Society 22 (2002) 1411–1424

www.elsevier.com/locate/jeurceramsoc

Monolithic and composite ceramic machining flaw-microstructure-strength effects: model evaluation

Roy W. Rice*

5411 Hopark Drive, Alexandria, VA 22310-1109, USA

Received 6 August 2001; accepted 1 October 2001

Abstract

A model giving the size, c, of flaws from machining of ceramics as $c \propto (E/H)^{1/3}(F/K)^{2/3}$, where $F=$ the vertical force on abrasive particles, and H, K, and $E=$ respectively local values of hardness, fracture toughness (i.e. small crack values) and Young's modulus is shown to be consistent with material, microstructural and machining parameter effects on flaws and strengths. Specifically this model is consistent with effects of machining flaw sizes on strengths due to effects of: (1) porosity and grain size in monolithic ceramics, (2) matrix grain size, and dispersed particle size and volume fraction in ceramic particulate composites, and (3) machining parameters such as grit size in monolithic and composite ceramics. Such a model emphasizes the role of microstructural and compositional dependence of properties impacting strengths via both flaw introduction as well as via flaw propagation to failure, which provides a broader perspective on strengths of typically machined ceramics. © 2002 Published by Elsevier Science Ltd.

Keywords: Composites; Flaws; Machining; Microstructural effects; Strength

1. Introduction

1.1. Brittle fracture and machining flaw model used

The uniaxial tensile strength of brittle ceramics is controlled some by loading conditions and especially by microstructure, flaws, and their interrelation. Of particular interest are flaws from abrasive machining process, especially diamond grinding, since it is often necessary to meet component dimensional and surface finish requirements, but is the major source of failure causing flaws in well made dense ceramics, as well as a number of porous ceramics, especially those with fine, uniform porosity. Thus machining, though often giving acceptable strength levels and reproducibility, needs better understanding, especially in terms of material, microstructural, and machining parameters that control the size and character of resultant machining flaws, as well as residual stresses introduced. This paper addresses primarily microstructural and machining parameters not addressed in other complimenting work.[1–4]

The most extensively used approach to determine machining flaw sizes from machining and related microstructural dependence of tensile strength has been via the Griffith or Irwin forms of the equation for tensile strength (σ) failure by brittle fracture:

$$\sigma = Y(2E\gamma)^{1/2}c^{-1/2} = YKc^{-1/2} \quad (1)$$

where $Y=$ a factor for the shape and location of the flaw causing failure, $E=$ Young's modulus of the body, γ its fracture energy, $c=$ the flaw size (commonly the depth, e.g. radius of a half penny flaw), and $K=$ the fracture toughness ($=(2E\gamma)^2$). Thus, by measuring both σ and K or γ and E, c can be calculated assuming a value for Y (which varies by a factor of < 2 for most flaws). However, this approach, while often useful, has important limitations, e.g. the flaw size calculated is the final, not the original flaw, size, i.e. after any subcritical crack growth, and neglects any residual, e.g. surface, stresses. Further, such c values do not differentiate between microstructural effects on the generation of the flaw during machining versus those on crack growth prior to failure. Also, measurement of K with large cracks, where significant increases in toughness may occur with

* Tel.: +1-703-971-4379.
E-mail address: roywrice@aol.com

0955-2219/02/$ - see front matter © 2002 Published by Elsevier Science Ltd.
PII: S0955-2219(01)00488-5

increasing crack propagation, leaves the issue of whether such large crack effects are operative at the orders of magnitude smaller machining flaw sizes and thus a factor in controlling failure.

More fundamentally, calculating c via Eq. (1) does not meet the important test of self consistency, i.e. where all 4 factors of σ, K, and c and Y are separately determined and compared for their consistency with one another. Inconsistent results are indications of other variables such as other, e.g. residual stresses from machining, (entailing both their level and spatial extent relative to flaw depths, both of which may be factors needing independent measurement, or of microstructural stresses, e.g. from thermal expansion differences between grains.[5] Also, while now discounted as a major factor in strength behavior of machined ceramics, stress concentrations from machining induced topography may be a more modest factor to be considered in some cases.[6] Much attention has been focused on understanding the microstructural dependence of strength via the microstructural dependence of K, especially with R-curve effects, but this neglects and may overshadow possible microstructural dependence of c and resultant effects on strength. Fractography to identify and characterize machining flaws, i.e. directly determine their Y and c values and their relation to the microstructure though very valuable, as shown below, is grossly under used.

An important additional aid in machining studies are models of the machining process, which have been derived from indentation mechanics to address 3 related aspects of machining. The first is the actual material removal process modeled by Evans and Marshall[1–3] based on lateral crack development from abrasive particles indenting the surface being machined. Such modeling gives good agreement with experimental data for horizontal and vertical grinding forces as well as for material removal rates, despite the idealizations made.[1–4] In both cases the dominant material (and microstructurally dependent) properties impacting the process was the product $K^{1/2}H^{5/8}$ to different exponents (8/9 for machining forces and -1 for material removal rates, H = hardness). Besides their value for modeling machining forces and rates, and corroborating machining flaw size and stress modeling discussed next, such models show a role of hardness in machining, as noted further below.

Indentation mechanics has also been used to model machining flaw sizes introduced, based on the formation of median cracks, and residual stresses on them[1–4] hence, resultant strengths, usually combined in a single model, which present two problems. The first is uncertainty based on idealization of the process, e.g. using a symmetric quasi-static indentation analysis for the dynamic, asymmetric machining process from abrasive particle motion and effects. Second, such combined flaw-residual stress models leave the sources of variability or uncertainty difficult or impossible to determine between which are due to machining effects via flaws or residual stresses, e.g. effects of surface heating in machining which can effect either or both. This problem is compounded by the fact that there are limited data on machining stresses and that almost all, or none, of it is accompanied by detailed flaw data. However, Marshall[2,3] gives a model for c alone, i.e.:

$$c \propto (E/H)^{1/3}(F/K)^{2/3} \tag{2}$$

where F = the vertical force on an abrasive particle, H, K, and E = respectively local values of hardness, fracture toughness (i.e. small crack values) and Young's modulus. This model, which avoids the uncertainties of combined models of flaw sizes and surface stresses, is the focus of this paper. The material and microstructural dependence of c via the 4 shown factors, when combined with Eq. (1) not only alters the dependence of strength on E and K, but also introduces a dependence on H. Also note that important effects of abrasive grit size on machining flaws and strength can be incorporated into Eq. (2) via F as follows. F is inversely proportional to the average number of abrasive particles active in machining at any time, which in the limit of no binder between abrasive particles, or with certain ratios of binder thickness between abrasive particles and abrasive particle size, is in turn inversely proportional to the square of the average abrasive particle size (d). Thus, for such conditions $F \propto d^2$, so $c \propto d^{4/3}$, and $\sigma \propto d^{-2/3}$.

The above model, and more extensively the combined flaw-residual stress, have been shown to be consistent with overall trends.[1–4] This paper complements and extends these evaluations by reviewing the machining, material and especially microstructural dependence of machining flaw size trends via Eq. (2) and on resultant σ. While Eq. (2) is generally only qualitative or semi-quantitative, it gives microstructural strength and flaw size dependences consistent with observations. Pertinent background on machining flaws and strengths is first summarized, then an application of Eq. (2) to the porosity and grain size, as well as effects of abrasive grit size dependence of machining effects in monolithic ceramics, are considered. Residual stresses from machining and their effects are also noted. This is followed by a summary review of effects of machining ceramic particulate composites and application of Eq. (2) as a function of machining and microstructural dependence of pertinent body properties. This focus on individual materials and factors gives added insight to the microstructural dependence of strengths of machined ceramics and ceramic composites, including a rationale for higher strengths in some composites, especially nanocomposites despite their frequently limited toughnesses.

1.2. Background on machining effects on flaw character and strength

The limited portion of ceramic studies having sufficient machining and material characterization provides insight to some general and specific machining trends and their consistency with Eq. (2).[5–20] Increasing grinding depth of cut, wheel speed, and infeed rate tend to give lower strengths, consistent with expected increases in F and thus c in Eq. (2). Fractography[6–12] shows general similarities of flaw character for fixed abrasive machining (sawing and especially grinding) and free abrasive machining (lapping and polishing), but with lower forces and finer abrasives and, hence, finer flaws for the latter as expected. However, a basic difference between these two types of abrasive machining is the collective, global directional paths of fixed abrasive particles versus the generally globally random directions of paths of individual free abrasive particles.

The above directionality of abrasive particles is a major factor in ceramic machining.[6–19] Fractography shows, as intuitively expected, median cracks form along, or very near, the apex of the groove formed by abrasive particles penetrating the surface with some possible variation in depth and continuity of the crack (Figs. 1 and 2). Such cracking along the groove is a stretched out version of the median crack of a static indenter, but with perturbations, mainly of continuity, due to stick-slip effects. The other, and often somewhat subsequent, cracking is basically transverse to the groove, similar to the other median crack of static indents nominally normal to the abrasive particle motion, but often with some curvature (Fig. 2). These transverse cracks also have variations, such as occurrence, type, and degree of curvature and in the separation of their halves on each side of the longitudinal crack (showing that transverse cracks form after the longitudinal cracks). These crack variations are mainly attributed to stick-slip phenomena in groove formation (beautifully shown in a movie[20]), which in turn is probably a factor in discontinuities and other variations in parallel cracks.

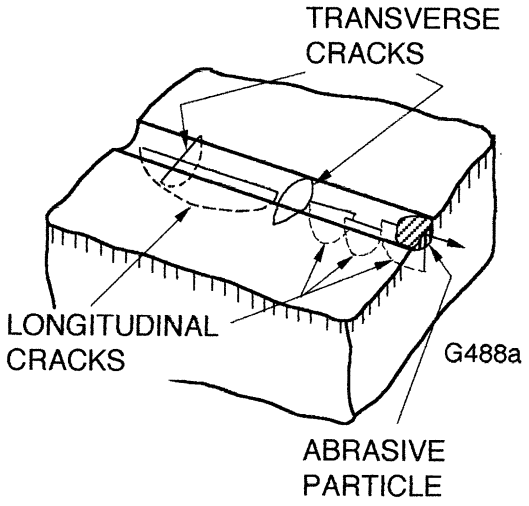

Fig. 1. Schematic of surface cracking generated from indentation of an abrasive particle into a surface being machined showing that the typical median cracks normal to the surface and each other formed around hardness indents occur in modified form in machined surfaces. The key modification from static indentation flaws is the elongation of the median cracks emanating into the body from the base of the groove formed by the abrasive particle's motion, and parallel with the groove and abrasive particle direction, as on the left side of the sketch. Frequent further modifications are: (1) the above elongated cracks being made up of a series of smaller segments and (2) the more half penny shaped cracks nominally normal to the elongated cracks, and the machining grooves and machining direction, often have various curvature, e.g. shown near sketch centre.

Despite variations, there are two important aspects of these machining flaws. First, both sets of cracks are generally of similar depths, which is fortitious since significant variations of their depths from one another and idealized median cracks might limit or preclude use of Eq. (2), which gives no clue to the asymmetry of the 2 machining flaw populations, but is not inconsistent with it. Second, a key difference between the above longitudinal and transverse cracks is their degree of elongation. Though this varies, it is the dominant factor in the strength anisotropy as a result of machining versus stress direction for fixed abrasive machining,[6,7] as shown by studies of glasses, single crystal and polycrystalline bodies.[8,12] Besides corroborating substantial earlier work, more recent studies have mapped out the strength transition between the two extremes of parallel versus perpendicular machining, e.g. as reviewed by Rice,[15] but there is no model, e.g. of mixed mode fracture for this strength transition as a function of stress versus machining direction, for fixed abrasive machining. Similar flaw elongation along abrasive particle grooves occurs with free abrasive machining, but the essentially random paths of the individual abrasive particles relative to one another precludes any overall directionality of the resultant strengths. Instead, failure of specimens with free abrasive finishing is controlled by elongated flaws along abrasive grooves, some of which are always normal to applied stresses to cause failure.

Three other overall aspects of machining flaws should be noted. The first two, again revealed by fractography, are that flaw sizes do not change significantly for typical machining, (1) of various typical ceramics and (2) as a function of grain size. With regard to the first point, most machining flaw sizes for strengths representative of many production ceramics are in the range of 20–60 μm, often the same range as for other flaws such as isolated pores.[5,21] Finer machining flaws $\sim$5–20 μm in size have been identified for higher strength, e.g. $>$ 600 MPa, fine grain bodies such as Si_3N_4.[22–24] A key result of flaw sizes not changing much with grain size is that machining flaws change from being larger than the grains at fine grain sizes, to smaller than larger grains in large grain bodies (and also often in isolated large grains).[11,17,19,25] This transition in flaw size relative to grain size is a major factor in a key change in strength-

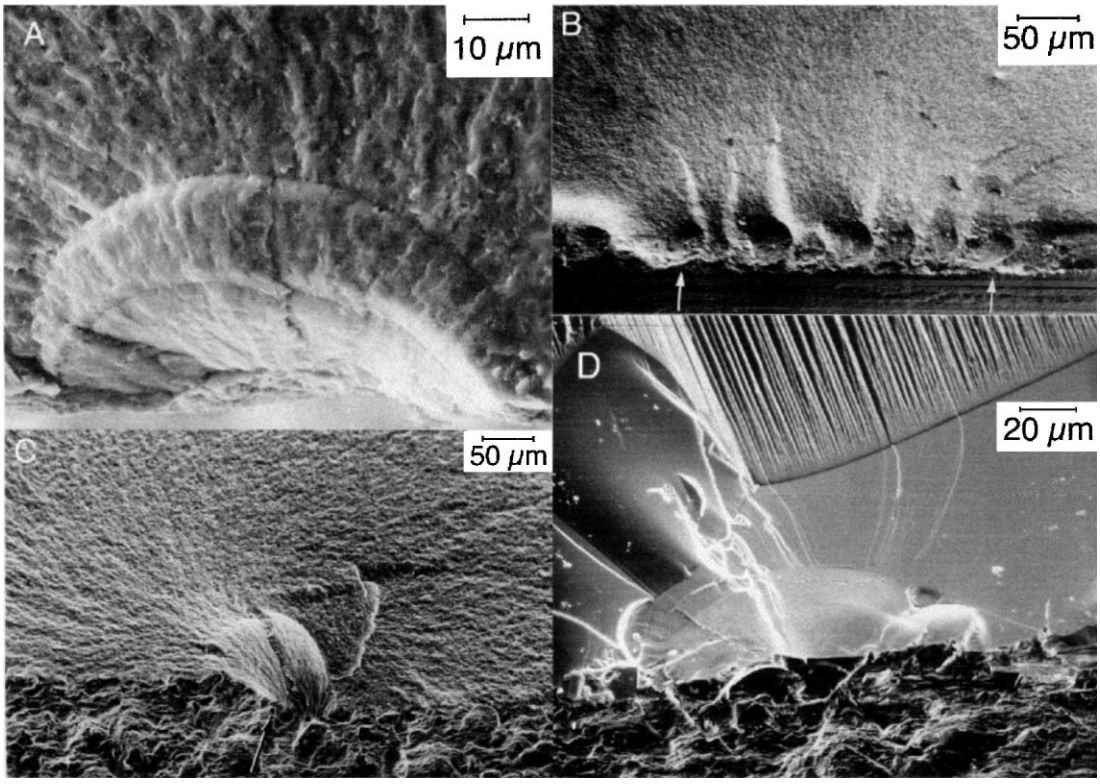

Fig. 2. Examples of actual machining flaws at fracture origins of dense, polycrystalline machined specimens illustrating their general character and some of their variations. (A) Flaw normal to the grinding direction in dense, fine grain $MgAl_2O_4$ indicating 2 or more stages of development (circular demarcations which are common, but far from universal) and greater than usual deviation from normality to the machined surface and some curvature to the final section. (B) Flaw parallel with the machining direction in a dense, optical grade MgF_2 showing substantially more than normal interruption and re-initiation of the crack along the abrasive groove. (C) Flaw partly parallel and partly approaching normal to the abrasive groove in dense, fine grain mullite, reflecting a combination or hybrid of the 2 basic machining flaw types. (D) Flaw parallel with the machining direction in a dense, large grain transparent Y_2O_3 showing common, but somewhat less than average elongation. Note that it is entirely contained in a single grain, but close to the left boundary of the grain and that such large surface grains are often truncated substantially, thus varying the apparent size of such grains.

grain size behavior (Fig. 3, as discussed later). The third overall aspect of machining flaws is that their size correlates with hardness, as do both machining forces and rates.[26] Thus, Munro and Freiman[27] surveyed fracture toughness and strength values of various ceramics, plotting fracture toughness versus tensile strength of various individual compositions of polycrystalline bodies at either constant grain size or constant porosity. It is shown here that the slopes of these plots, which are the proportional to the inverse of the average flaw size for a given material correlates with representative hardness values for dense bodies of each composition (Fig. 4).

2. Comparison of machining flaw size predictions with strength-flaw-microstructural effects in monolithic ceramics

2.1. Effects of porosity on machining flaws and strength

The porosity dependence of tensile strengths of machined ceramics, especially where pore sizes are substantially smaller than machining flaws so individual pores or clusters of pores are not common fracture origins, is generally very similar to, but often somewhat greater than, that for Young's modulus.[17,18,28,59] Eq. (1) shows that, baring toughening effects such as crack branching or bridging, the porosity dependence of strength, toughness and Young's modulus (E) should all be the same since theoretically the porosity dependence of γ is normally that of E, i.e. close to broadly observed trends.

The machining flaw model [Eq. (2)], is approximately to very consistent with this correspondence of the porosity dependence of strength and Young's modulus (E), since the porosity dependence of E and H are the same, hence, canceling in their effect on flaw size. Thus, in the worst case the flaw size dependence on porosity is that of the normal, i.e. small, crack toughness raised to the $-2/3$ power, so the net porosity dependence of strength would be the K porosity dependence raised to the $+4/3$ power, i.e. 1/3 of this due to porosity effects on c via Eq. (2) and the other 3/3 due to the K dependence of strength via Eq. (1). Such a net porosity dependence of

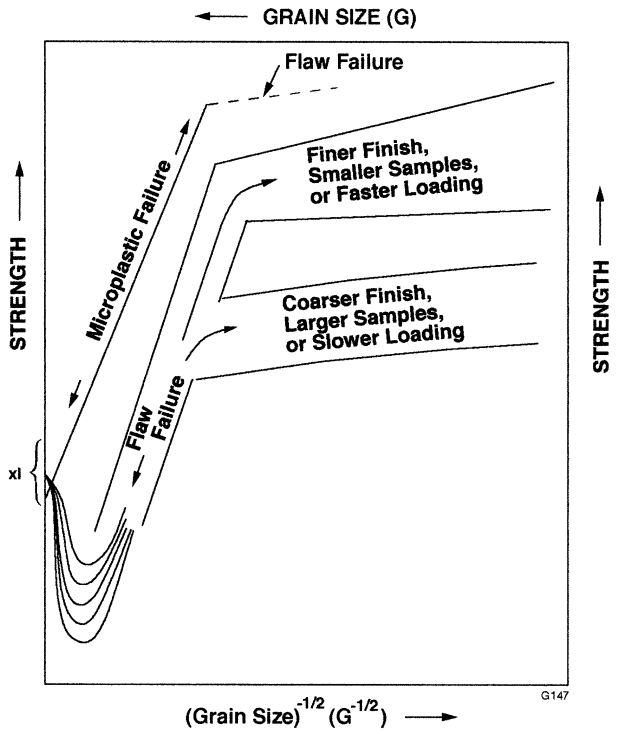

Fig. 3. Schematic of the typical strength dependence as a function of $G^{-1/2}$ (G = grain size), where strength is controlled by machining flaws. The finer G branch reflects flaws sizes $> G$ and the larger G branch flaws sizes $\leqslant G$, meeting when $2c \sim G$.

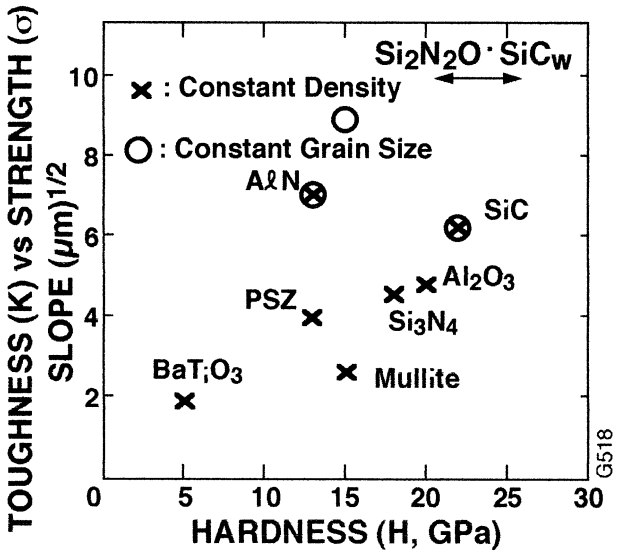

Fig. 4. Plot of the slope of plots of fracture toughness versus tensile strength of various individual compositions of polycrystalline bodies at either constant grain size or constant porosity versus representative hardness values for dense bodies of each composition. Note that $K/\sigma \propto c^{-1/2}$, increases with increasing H, consistant with Eq. (2). Plot obtained from evaluation of data compiled by Munro and Freiman.[27]

strength via effects of K on c and directly on K is reasonably consistent with data which shows the porosity dependence of strength being $\geqslant$ that of E or K (from small crack tests) since E and K have equal porosity dependences. Whether the porosity dependence of c is fully reflected in that of E, H, and K, or there is also some direct effect of porosity via F is uncertain. Clearly the force (F) on each abrasive particle depends on the stiffness of the body being machined, but whether this is fully reflected in the porosity dependence of E is uncertain, e.g. porosity may aid fragmentation of swarf, reducing F. However, direct measurement shows the machining difficulty (M_D, i.e. the reciprocal of the machining rate, M_R) decreases as porosity increases the same or somewhat $< E$ decreases with increasing porosity.[26] Since faster machining implies lower forces resisting machining, i.e. that $F \propto 1/M_R \propto M_D$ and thus that the porosity dependence of strength via Eqs. (1) and (2) is the same or slightly $>$ that of E.

The one study of porosity-machining effects on ceramic strengths,[15,17] supports the above general effects of porosity on strength. It showed by direct fractography that machining flaw sizes in fine grain porous Al_2O_3 were the same or similar to those in fine grain dense Al_2O_3 and that toughness values calculated from the flaw dimensions showed the same or similar porosity dependence as for strength and E. This correspondence of machining flaws in bodies that were otherwise about the same except for different amounts of fine porosity, was also shown by the anisotropy of strengths as a function of machining parallel or perpendicular to the stress axis of strength testing, generally being independent of the amount of porosity. The limited exceptions to this independence of strength anisotropy as a result of machining direction as a function of porosity were some cases where strengths of specimens ground perpendicular to the tensile axis showed reduced dependence of strength on porosity at higher porosity levels. The extent of this reduction was observed to increase as the heterogeneity of the spatial distribution of the porosity increased, indicating increasing porosity heterogeneity progressively limited elongation of flaws formed along abrasive particle paths.

2.2. Effects of grain size on machining flaws and strengths

The grain size (G) dependence of tensile strength of machined bodies has been extensively shown to be a direct result of machining flaw interaction and resultant relation to grain size.[11,15,19,25] The dependence of strength on G over the normal G range encountered has two regimes, a finer G regime where strengths generally show modest decreases as G increases and a larger G regime where strengths decrease substantially faster as G increases (Fig. 3). The finer G regime may follow various, generally parallel paths, or branches, that depend on machining parameters, e.g. grit size as discussed below, or a single broader branch reflecting

greater flaw variations. In contrast to possible wider or multiple finer grain branches there is a single larger G branch. This two branch behavior has been shown to be due to machining flaws typically being larger than finer grains and not varying much with G, e.g. being similar in single crystal specimens for the same machining condition. Thus, as G increases in a given material, the size of machining flaws introduced must first approach, then equal, and subsequently become progressively less than the grain size (in terms of actual sizes since they have different measures in practice, i.e. G is measured by a diameter and c by a radius). Thus, the larger and finer G branches meet when the flaw and grain sizes are the same, which actually encompasses a range of G due to statistical size variations of both the machining flaws and grains. The larger G branch reflects machining flaws being contained in or around part of a single grain whose size becomes the flaw size and where flaw propagation is controlled by grain boundary or single crystal toughness values or their transition to polycrystalline values. This larger versus finer strength change and the transition between single and multiple grain toughness values, which has been modelled,[29–31,59] is a basic reason why many larger crack toughening effects often have no effect on strengths, since strengths at larger grain sizes are no longer determined exclusively, if at all, by polycrystalline toughness values, which reflect R-curve effects when they occur.

Three facts should be noted about the above flaw and strength trends. First, strengths generally decrease as machining grit size increases, mainly or exclusively at finer G, i.e. at larger G there is much less, if any effect of grit size on strength, as discussed in the next section. Second, while some have claimed that the slopes of the finer G branches are zero, there is no data which conclusively shows this and there is substantial data to the contrary.[19,25] Increasing impacts of microstructural stress from thermal expansion anisotropy in noncubic materials and of elastic anisotropy in all crystalline ceramics as G increases have been cited as reasons for the limited strength decrease as G increases along finer G branches, but this has not been established. Such strength decrease as G increases along finer G branches have also been attributed, at least in part, to microstructural effects on machining flaw generation as also discussed below. Third, not only do flaw sizes not vary significantly with G, they generally do not vary significantly over a variety of different ceramic materials, e.g. note that most ceramic strength-G behavior falls in a limited range.[19,25]

Both the limited strength decreases as grain size increases over the finer grain branch and the limited flaw differences for many ceramics can be seen from microstructural effects per Eq. (2). For a given material E does not depend on G unless there is microcracking or some other special mechanism operative (in which case machining flaws and their effects on strength are modified, or preempted). However, H clearly depends on G, generally decreasing as G increases,[19] which thus gives a modest increase in flaw sizes, hence modest strength decreases as grain size increases over the finer grain branch as observed. K may also depend on G, but the local, small crack values of K pertinent to machining flaw generation do not appear to have much G dependence, but if they do they are likely to increase modestly as G increases over the G range of finer G branches, counteracting at least some of the effects of H increasing with decreasing grain size on flaw size. Thus, the clear, but modest decrease in H, hence increase in c, as G increases provides another source of a modest strength decrease as grain size increases over the finer grain branch and possible modest changes in K provide a rational for variations in this slope. However, large K increases as G increases due to R-curve effects with large cracks are clearly inconsistent with the modest slopes of finer G branches. Turning to the limited flaw size differences for different materials, note that hardness overall roughly correlates with E, so differences for different materials tend to cancel out. This combined with limited small crack K values for many ceramics gives a limited range of flaw sizes per Eq. (2) consistent with fractographic observations.

The original, extensive demonstration of strength anisotropy as a function of machining versus tensile stressing directions noted a G dependence of such anisotropy in MgO, but did not address this on a broader basis.[7] However, subsequent consideration of the original along with added data shows a broad substantial grain size dependence of the strength anisotropy as a function of machining versus stressing direction[15,16] (Fig. 5). Thus, the range of materials investigated shows the anisotropy of strengths as a function of machining direction is highest at finer grain sizes, decreasing as G increases, disappearing at intermediate G, e.g. $\sim$ 50 μm, then increasing as G further increases to the limits found for single crystals. While the latter clearly depends on crystal orientation, strength anisotropy as a function of machining direction in single crystals is often a substantial fraction of those at fine G. The minimum of strength anisotropy at intermediate G is generally consistent in its occurrence and specific G values with the intersection of larger and finer G branches, again consistent with grains constraining flaws as the flaws approach the size of grains. As the strength anisotropy minimum is approached the lower strength finer G branch due to stressing normal to the machining direction rises as G increases, meeting the larger G branch where it meets the higher strength finer G branch from stressing parallel with the machining direction since the two basic machining flaw populations become the same due to being constrained by the individual grains. Also, note that both the grain size of the minimum of strength

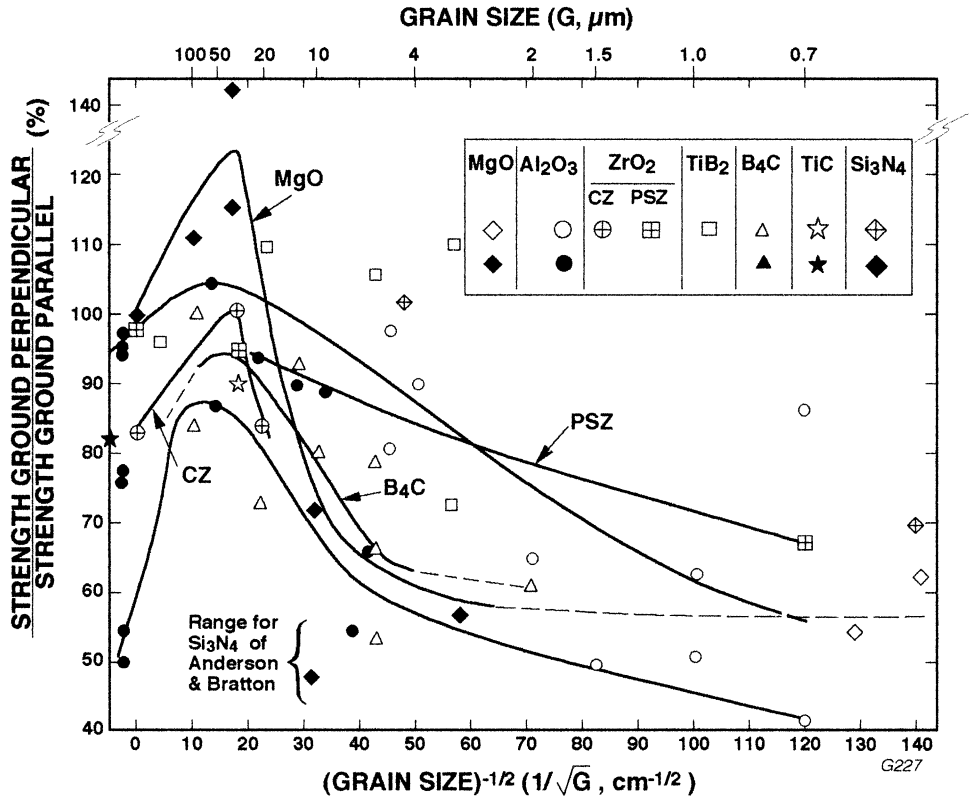

Fig. 5. Plot of the ratio of the strengths of various dense ceramics as ground perpendicular versus parallel to the test bar/stress axis versus the inverse square root of their grain sizes (for ready comparison with typical strength-grain size plots, e.g. Fig. 3). This ratio reflects the anisotropy of strength as a function of machining direction versus the test bar/stress axis. Note that the anisotropy; (1) is greatest at fine grain sizes, but despite dependent on crystallographic orientation of single crystal specimens, can also be substantial in them, and (2) generally disappears, i.e. at a ratio of 100% at grain sizes in the range of 20–100 μm. (MgO exceeding 100% is attributed to strengthening of larger grain bodies due to surface work hardening from finishing.) After Rice.[15,16]

anisotropy and the intersection of finer and larger G strength-grain size branches are approximately the same, and also correlate, at least approximately with the frequent minima found for most hardness values.[19]

2.3. *Effects of machining grit size and direction on strength and machining flaws*

Consider now effects of machining grit size on resultant machined ceramic strengths. As noted earlier extension of the machining flaw model predicts a limiting dependence of strength on grit particle diameter (d) of the order of $d^{-2/3}$. The limited data available (mostly for bodies with $G \sim 1$–10 μm) indicate consistency with this (Figs. 6 and 7). Somewhat more data exist for dense sintered or hot pressed Si_3N_4,[32–34] all of which show trends reasonably consistent with the model and generally with each other, and between strengths from machining parallel or perpendicular to the tensile axis of strength testing. The limited characterization of the material and grinding parameters (often only the grit size was given) preclude indicating possible sources of the differences in the data, mainly of Ota and Miyahara,[34] for grinding parallel to the bar axes. More recently, Mayer and Fang[35] reported that the difference in strength of Si_3N_4 as a function of machining direction is reduced, then disappears as the grit size increases, e.g. respectively at 80 and 50 grit. Data of Kishi et al.[36] for β-sialon shows extension to finer grit sizes, but possible variations of it at very fine grit sizes (e.g. 6000, Fig. 6), which may reflect changing indent-cracking effects when the indent (related to grit) sizes are similar.[19] Strengths of SiC ground normal to the bar tensile axis with various grit sizes showed similar trend over a range of grain sizes to that for some Si_3N_4 results.[37]

Turning to the limited data for oxides (Fig. 7), data of Bradt and colleagues on hot pressed MgO[38] and Al_2O_3[39] (both for perpendicular grinding) agree reasonably with the model and with their SiC data reflecting the similar techniques and resultant consistency. Data of McKinney and Herbert[40] are also reasonably consistent with the model and the other Al_2O_3 data despite being with SiC abrasive in lapping instead of grinding and in biaxial flexure versus uniaxial flexure testing. (Note that the latter consistency is reasonable since, as noted earlier, biaxial tests of lapped specimens effectively reflect strengths similar to those of specimens tested with uniaxial tensile stress normal to the grinding

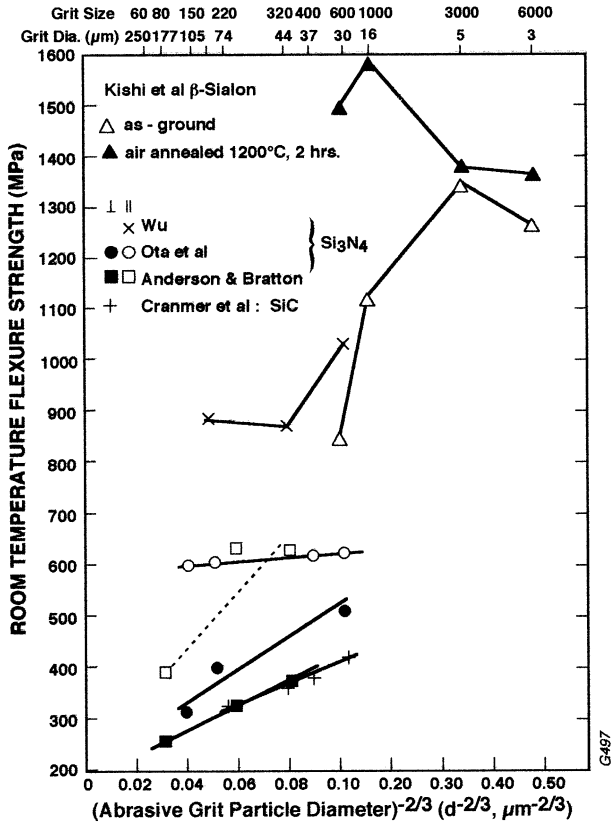

Fig. 6. Flexure strength for diamond grinding flexure bars parallel or perpendicular to the bar axis for dense sintered or hot pressed Si_3N_4[32–34], β-sialon,[36] and SiC[37] versus the abrasive particle size to the minus two thirds power, per Eqs. (1) and (2). Note strengths for as-machined and for an β-sialon, the latter effects of both some changes in machining stresses and stresses introduced from surface oxidation.

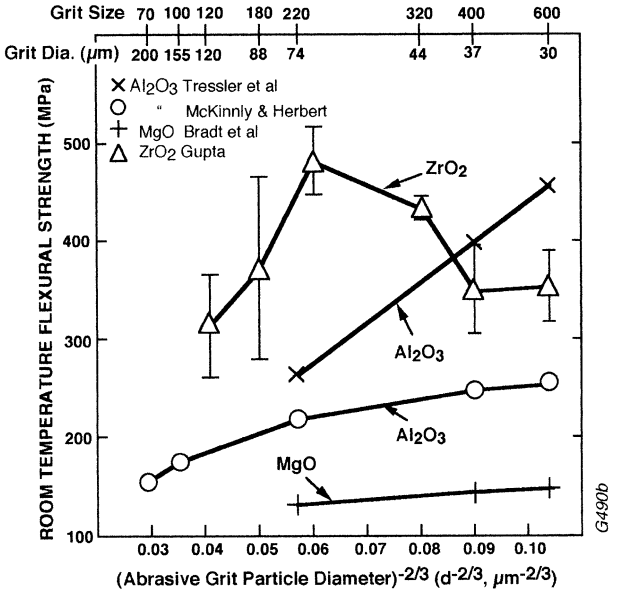

Fig. 7. Flexure strength of hot pressed MgO[35] or Al_2O_3[36] and commercial 96% Al_2O_3,[40] as well as sintered TZP[41] (composition and grain size not given) disks versus the abrasive particle size to the minus two thirds power, per Eqs. (1) and (2). Note that the hot pressed MgO and Al_2O_3 were diamond ground perpendicular to the bar axis, while the 96% Al_2O_3 and sintered TZP were respectively lapped and ground with SiC abrasives and tested in biaxial flexure (as-fired strengths of the ZrO_2 were 354±36 MPa).

direction.) The data for a TZP[41], which also used SiC instead of diamond abrasive and biaxial versus uniaxial flexure, are reasonably consistent with other data at coarser, but varies at finer, grit sizes. Gupta[41] suggested that the changing trends of his data reflected changing surface stresses, but no data were given in support of this. Except for some variation at finer grit size, there is general agreement of overall trends of strength decreasing, hence flaw sizes increasing, as abrasive grit sizes decrease (hence grit diameter increases). This trend occurs despite variations between various tests, some of which reflect varying (uncited) machining parameters such as abrasive concentration/binder content and depth, direction, and speed of cut. Note again, however, that effects of coarser grit sizes on strengths become much less or disappear as the flaw size approaches the grain size, consistent with larger grains constraining flaw sizes. Also note that the clear correlation of strength with the grit size where $2c < G$ implies that strength correlates with machining flaw sizes, not with *R*-curve or other increases in toughness in toughness tests of some bodies with large cracks.

2.4. Comparison of calculated and fractographically observed machining flaw depths

Now consider direct evaluation of flaw sizes (depths) calculated from Eq. (2) (using representative values shown in Table 1 and a proportionality factor of 1, similar to other evaluation[4]) versus actual measured machining flaw depths obtained from fracture origin determinations of flexure bars using data from previous publications[6–19] and some from more recent tests. Results for machining parallel as well as perpendicular, and for some unspecified machining directions, while scattered, show some correlation between observed and calculated flaw depths (Fig. 8). The lack of a 1 to 1 correspondence of the observed and calculated flaw depths, beyond the unknown specific value of the proportionality factor in Eq. (2) and scatter, is attributed, in approximate order of expected decreasing impact, to: (1) use of a single number for the flaw size, i.e. a half penny radius (depth) rather than a more exact ellipsoidal flaw approximation, (2) some variations in machining conditions for different tests, (3) simplifications of the model, i.e. simple idealized flaws and uniformity of abrasive particle sizes and shapes, and spatial distribution and extent of penetration into the machined surface, (4) the limited amount and especially range of the data (e.g. no data for in situ toughened Si_3N_4), (5) uncertainties in (the local) *E*, *H*, and especially *K* values to use, and (6) effects of residual machining stresses.

Table 1
Material properties and calculated flaw sizes[a]

Material[b]	E[c] (GPa)	H[d] (GPa)	K[e] (MPam$^{1/2}$)	c[f] (μm)
Al_2O_3 pxl	400	21	3.5	115
Al_2O_3 sxl	400	21	2	168
TiO_2 sxl	280	13	1.5	211
Y_2O_3 pxl	165	8	1.2	244
TZP pxl	230	16	6	73
ZrO_2 pxl	230	16	3	140
ZrO_2 sxl	230	16	1.5	185
β-Al_2O_3 pxl	200	14	2.3	150
$MgAl_2O_4$ pxl	295	18	2.5	140
Mullite pxl	220	15	1.8	166
Soda lime glass	70	6	0.8	152
B_4C pxl	450	30	3	118
SiC pxl	400	25	3	121
TiC sxl	460	28	1.5	211
MgF_2 pxl	130	6	0.9	298

[a] Per Eq. (2) assuming the proportionality constant is 1 and that $F = 1$ N.
[b] Pxl = polycrystalline body, sxl = single crystal.
[c] Young's modulus.
[d] H = hardness.
[e] K = fracture toughness.
[f] c = flaw size (depth of half penny flaw).

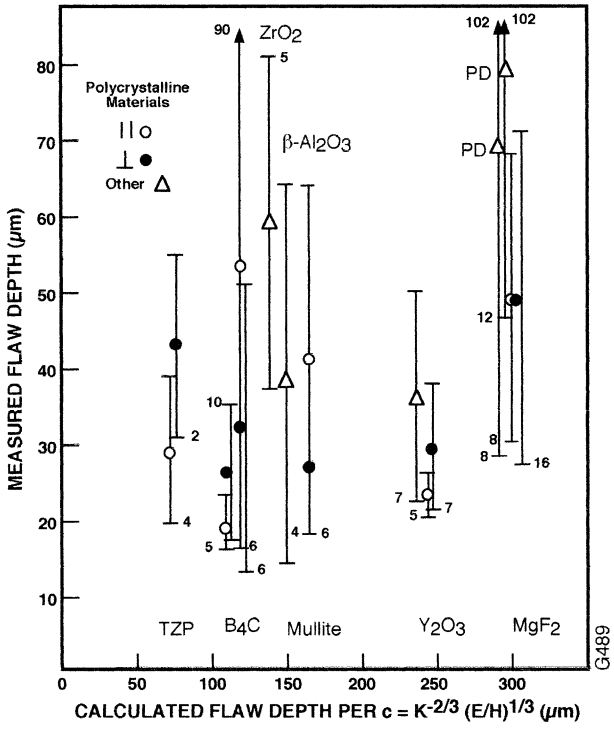

Fig. 8. Actual flaw depths from fractography of various polycrystalline ceramics versus those calculated per Eq. (2) using values shown in Table 1, a proportionality factor in Eq. (2) of 1, and a force (F) of 1 N. Note the individual body compositions shown for flaws from machining parallel (‖) or perpendicular (⊥) to the flexure bar axes and for other unspecified machining (other) and the number of measured values averaged (sub- and super- scripts) and the standard deviations (vertical bars). Additionally, two sets of optically polished MgF_2 discs tested in ring on ring biaxial flexure are shown, designated by PD.

Similar evaluation of the much more limited data for single crystals (mainly of Al_2O_3, TiO_2, and $MgAl_2O_4$) showed similar trends, but with even more emphasis on factors 4 and 5 above.

Beyond the above data showing some consistency with the model based on observed versus calculated flaw sizes, note that the calculations indicate reasonable levels of loads and stresses on abrasive particles. Thus, calculated flaw sizes are of the order of 3 times observed values. Setting the 2 flaw sizes equal, and still assuming a modest proportionality constant of 1, implies the force, F, on abrasive particles is of the order of 0.2 N, which would translate to stresses averaged over individual abrasive particles of 500 MPa to ~ 2 GPa.

2.5. Residual machining stresses

Finally consider effects of residual surface stresses from machining. Though detailed studies have been limited, and quantification can be complex due, for example, to multiaxial stresses and stress gradients, they clearly show that machining typically results in a surface compressive stress.[42–48] Thus, earlier data of Hanney and Morrell[42] showed that 320 grit diamond grinding of 95% alumina bars resulted in surface compressive stresses of ~ 30 MPa. More recent and comprehensive tests of Johnson-Walls[45] showed that residual surface stresses from 240 grit diamond grinding with shallow (2 μm) depths of cut of 8 ceramics (e.g. As_2S_3, ZnS, MgF_2, a ferrite, Mg-PSZ, and Si_3N_4, along with some Al_2O_3) generally increased nonlinearly as the hardness of the machined ceramic increased. While there were variations with soda-lime glass and Si crystals falling somewhat below the trend and Si_3N_4 and especially PSZ, being higher, results were essentially the same whether specimens were ground parallel or perpendicular to the test bar axes. Increasing depths of cut to 10–20 μm did not give significant changes in surface stresses, and a strength decrease of only ~ 5%. The depth of the compressive layer was estimated as ~ 10 μm in Si_3N_4 at a stress level of ~ 350 MPa. Single point diamond machining of Si_3N_4 by Kirchner and Isaacson,[49] which gave flaw depths of 10–50 μm, showed surface compressive stresses of the order of 100–200 MPa.

Samuel et al.[46] also studied a Ni–Zn ferrite, a TZP, and 2 dense Si_3N_4 bodies showing that compressive surface stresses from 400 grit diamond grinding (with a 200 μm depth of cut) extended to 10–20 μm below the surface (flaw depths based on calculations from strengths and toughnesses were similar at 8–20 μm). These stresses were up to ~ 25, 450, and 300–400 MPa in respectively the ferrite, TZP and Si_3N_4, with stresses from grinding parallel versus perpendicular to the bar axes generally being the same, except in the ferrite where stresses for grinding perpendicular were ~ 2 those for parallel grinding. They noted that the apparent (calcu-

lated) flaw depths in the ferrite were substantially effected by the residual stresses. Chou et al.[50] reported surface compressive stresses varying from ~ 60 to ~ 500 MPa in a fine (2–3 μm) grain Al_2O_3 that extended ~ 10 μm deep in the samples. Surface stresses have also been noted from machining ZrO_2 toughened alumina due to transformation of the zirconia.[51]

In summary there is substantial evidence of surface compressive stresses in machined monolithic ceramics, with more limited data showing such stresses being a fraction, e.g. 1/10 to 1/2, of strength, with the higher fractions being for TZP and Si_3N_4 which typically have higher machined strengths. Depths of such stresses are indicated as a fraction of the normal flaw depth, but may approach 100% of flaw depths in some cases. Thus, combined effects of the magnitude and depth of surface machining stresses appears to most commonly cause variations in strength-machining flaw relations, but in some cases such stresses may substantially alter them.

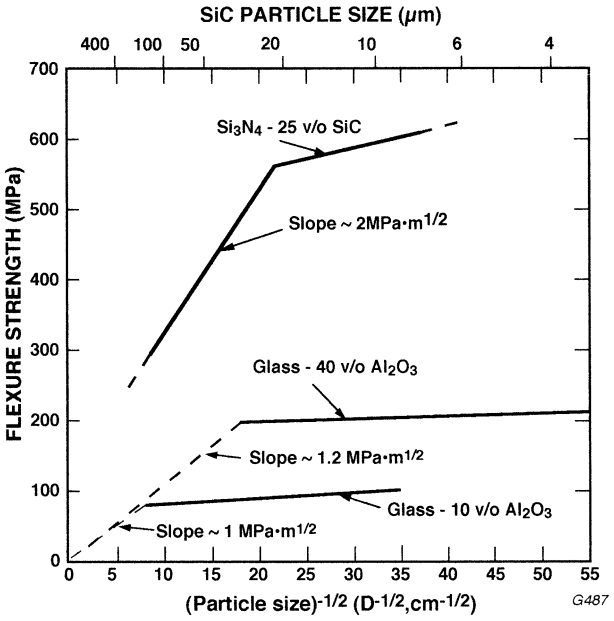

Fig. 9. Examples of the tensile (flexure) strength $-D^{-1/2}$ dependence for ceramic particulate composites where D = the diameter of the dispersed particles. Data after references 55,56, see also Ref. 19.

3. Machining effects on flaws, surface stresses, and strengths of ceramic particulate composites

Much less study of machining of ceramic composites has been conducted, but there are sufficient data to show close and expected parallels with machining behavior of monolithic ceramics. A major factor supporting the direct parallel of machining flaw effects on strengths of monolithic ceramics is the recently demonstrated dependence on particulate composite strengths on the dispersed particle size (D), i.e. a $D^{-1/2}$ dependence for such composites directly paralleling the $G^{-1/2}$ dependence for monolithic ceramics[19] (Fig. 9). Thus, there is one or more finer particle branches (depending on machining variations) where strengths decrease slowly as D increases due to effects of changing particle (and matrix grain) size on H and K values in Eq. (2). This is followed by the single larger D branch where machining flaw sizes along or within dispersed particles are $\leqslant D$, so over a range D becomes the flaw size, with the resultant greater dependence of strength on D. Again the two branches meet when the flaw and particle dimensions are about equal (recognizing that they are respectively characterized by a radius and a diameter, and the statistical variations involved), and the slopes of the larger D branch are typically $<$ the composite toughness due to transitions between the latter and dispersed single crystal particle or interfacial values.

Though limited, other data for machining effects on composites (mostly for the finer particle size branches corresponding to the finer grain size branches for monolithic ceramics, which for both are where most of the practical interest, and greatest effects are) shows similar effects as seen for monolithic ceramics. Thus, strengths increase as grit size decreases, e.g. Wahi and Ilshner[52] demonstration of increased strengths in Al_2O_3–TiC particulate composites with polished versus ground surfaces. Similarly, Rice's fairly extensive and most recent study of machining direction effects on monolithic and composite ceramics shows that a variety of particulate composites, including Al_2O_3–ZrO_2 and Al_2O_3–TiC, as well as Al_2O_3–SiC whisker composites have the same or similar strength anisotropy versus machining direction as for monolithic ceramics.[15] The primary, and probably only difference is that the composites often show less anisotropy of strength as a function of machining direction, but primarily or only in proportion to the extent of failure initiation from larger processing defects instead of machining flaws.

There has been no known specific identification and characterization of machining flaws introduced in ceramic composites, in part due to lack of attention and probable frequent greater difficulty in detecting them because of lack of fractographic clarity. However, 5 observations beyond the above similarities of machining effects on composite strengths show that machining flaw character in ceramic particulate composites is controlled in the same fashion as for monolithic ceramics. The first observations is the generally lower strengths (despite high toughnesses) of platelet composites[19] and their frequent failure from larger interfaces between platelets and the matrix, which are likely locations for machining flaws controlling strengths. Second is the dependence of flaw depths on the factors in Eq. (2) via compositional, and especially microstructural, effects on E, H, and K. Thus, while increasing matrix grain size and increasing dispersed particle size increase large crack toughness

values, inconsistent with strengths decreases, Eq. (2) predicts increased flaw sizes consistent with observed strength decreases. Note that this is also true for nano composites, which often show no increase in K, but increases in H consistent with increased strengths from expected reduced flaw sizes via Eq. (2). The third through fifth observations are similar calculated sizes of machining flaws introduced in, and controlling strengths, of ceramic composites, the similar compressive stresses from machining composite[50–52] and monolithic ceramics, and especially the compositional effects on composite flaw size and composite strength dependence on dispersed particle sizes, as discussed below.

A previous study by Rice[19,54] showed a broad trend for the ratio of strength and toughness for a given composite to pass through a maximum as a function of the volume fraction of second phase. This strongly supports the thesis of this paper that body composition and microstructure effect the sizes of machining flaws introduced, e.g. per Eq. (2). Thus, such a strength/toughness ratio is $\sim c^{-1/2}$, within the uncertainties of flaw shape (typically a factor of ~ 2), so a minimum of flaw size is shown at intermediate volume fractions of dispersed phase (ϕ). Such flaw size minima are expected from Eq. (2) since both small and large crack values of K for composites show maxima at intermediated ϕ, but 2 factors should be noted. First, high toughness values from large crack tests generally yield unrealistically large flaw sizes, e.g. mm instead of μm in scale. Second, maxima of flaw sizes as a function of ϕ may often be shifted some from that of K due to changes in E and H with ϕ per Eq. (2), though calculations of c from these values as a function of microstructure are often generally driven by microstructural dependence of K (Fig. 10).[19,54]

Note that the above results combined with other factors provide a possible explanation for the occurrence of higher strengths in some nanocomposites than expected

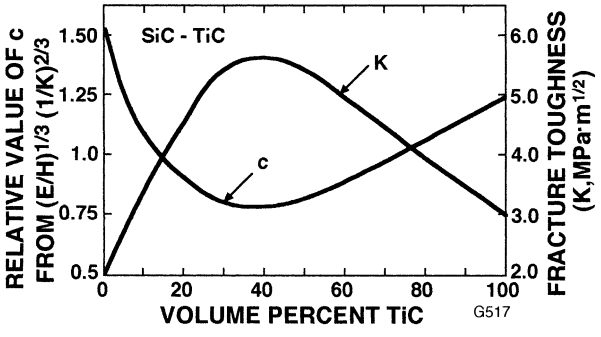

Fig. 10. Example of ceramic particulate composites showing a minimum of flaw size, c, as a function of composite composition using measured E, H, and K values of Endo et al.[57] showing some effects of E and H, but a dominance of K per Eq. (2) since E and H values for both the matrix and dispersed phase are both high, so there are limited changes with composite volume fraction composition. Such minima of c generally correlate with values indicated by strength and toughness per Eq. (1).

from their frequent modest toughness values.[50] Thus per Eq. (2) limited increases in K values reduce machining flaw sizes somewhat, but the typically substantially higher hardness values for such very fine grain composites further reduces these flaw sizes. Also note that ceramic composites can have significant surface compressive stresses from machining, e.g. 30–450 MPa extending to depths of $\sim$ 12 μm in alumina based nanocomposites similar to all alumina bodies similarly machined.[50] Thus net reduction of machining flaw sizes combined with effects of increased toughness on strength via Eq. (1) and the probable effects of considerable surface compressive stresses that can occur in such composites appear to provide a much better basis for understanding strengths of such composites than a singular focus on Eq. (1).

4. General discussion, summary, and conclusions

The overall thrust of this paper has been to expand the perspective on machining flaws that control strengths of well made ceramics, showing the traditional approach of using Eq. (1) as the only source of flaw size information is often inadequate. Both fractographically derived flaw information and modeling of machining flaw generation are important. A model for the dependence of flaw sizes on material and microstructurally dependent properties, i.e. local values E, H, and K impacting flaw formation, as well as key machining parameters such as grit size is valuable as shown in earlier work[1–4] and more extensively in this paper.

For monolithic ceramics this model corroborates observed strength decreases being about the same or somewhat faster with increasing amounts of fine porosity than for Young's modulus, by showing limited dependence of flaw sizes on porosity via its effects on E, H, and K. Similarly, overall the model shows limited differences of flaw sizes in different ceramics due to generally limited differences in the E/H ratio, but there is some trend with H due to materials with lower E/H ratios, e.g. H increases substantially from Al_2O_3 through SiC and B_4C, all with $\sim$ the same E value. Also, there is limited change in flaw sizes in a given material as grain size varies as observed experimentally and shown by effects of no changes in E and modest changes in H as well as no or modest changes in (small crack) K values as grain size varies with resultant limited impacts via the model. However, the persistent increase of H with decreasing G indicates a modest decrease in flaw sizes and thus a modest increase in strength as grain sizes decrease at finer G values. There may also be some modifications of flaws introduced when the machining grit sizes are about the grain size of the body being machined due to effects on indentation cracking when indent and grain sizes are about equal.[19,58]

Grain size of ceramic bodies also has other impacts on machining effects. One of these is significant changes in the strength anisotropy as a function of machining direction (Fig. 5). Another is via impacts on *R*-curve effects which occur to varying extents, i.e. increases with grain size (and intergranular fracture), but have not been correlated with machining effects. However, similar machining effects in TZP and silicon nitride, which often have substantial *R*-curve effects, and other ceramics imply limited or no of *R*-curve effect on machining effects on strength. Third is greater surface plastic deformation in machining at finer grain and grit sizes.[19] All of these factors, especially the first and third are probable sources of varying slopes in Figs. 6 and 7.

Turning to ceramic particulate composites, their same dependence of strength on dispersed particle size as found for monolithic ceramics with grain size, the same or similar dependence of composite strengths on machining direction and with machining grit size as for monolithic ceramics shows similar machining flaw formation in both types of ceramics. This correspondence is also shown by the persistence of a minimum in machining flaw sizes at intermediate composite compositions, due mainly to a maximum in *K* values, but shifted some by differing, usually more modest, dependences on changes in *E* and *H* with changing composite composition (Fig. 10). Such *K* effects on machining flaws in ceramic composites is a particularly important example of strength benefits of *K* increases via both its effects on flaw formation, i.e. reducing the size of flaws from machining, as well as in increasing the resistance to their later propagation to failure. Strength correlations with the small scale of machining flaws in ceramic particulate composites also implies that there is limited, if any, *R*-curve effects, as observed with larger scale crack propagation, as noted above for monolithic ceramics. However, more testing is needed, especially bodies with high *R*-curve effects, with both machining grit size and machining direction effects providing key opportunities to scale flaw sizes for such tests of *R*-curve effects on strengths of machined composites, rather than implying effects from toughness testing with large scale cracks.

Evaluation shows that other sources of stresses, especially residual surface compressive stresses from machining can be sufficiently high in value and their depth to be a factor. Fractography can also be an important tool in indicating the level and depth of surface stresses via their impact on fracture mirror patterns.[13] Other sources of local stresses such as from miss matches in properties such as thermal expansion of grains in monolithic ceramics or grains and dispersed particles in ceramic composites may impact strengths of both machined monolithic and composite ceramics, but may be greater in ceramic composites. Both direct measurement of such stresses as well as assessing them via the more comprehensive approach addressed in this paper are important for a more comprehensive understanding of strength behavior.

Thus in summary, a model of flaw introduction in machining of monolithic and particulate composite ceramics as a function of their properties and microstructures provides a more comprehensive view of the resultant strength behavior. However, more testing is needed, focusing especially on interaction of machining flaws and residual stresses and *R*-curve effects using respectively more fractography and effects of machining grit size and direction.. Finally, more experimental study, especially via fractography, should allow improvement of such models, e.g. allowing improved correlation of measured and calculated flaw sizes beyond initial observations in Fig. 8.

Acknowledgements

Dr. David Marshall of Rockwell Science Center is thanked for comments on the manuscript.

References

1. Evans, A. G. and Marshall, D. B., Wear mechanisms in ceramics. In *Fundamentals of Friction and Wear of Materials, 1980 ASM Materials Science Seminar*, ed. D. A. Ringney. American Society for Metals, Metals Park, OH, 1981, pp. 439–452.
2. Marshall, D. B., Failure from surface flaws. In *Fracture in Ceramic Materials—Toughening Mechanisms, Machining Damage, Shock*, ed. A. G. Evans. Noyes Publications, New York, 1984, pp. 190–220.
3. Marshall, D. B., Evans, A. G., Yakub, B. T. K., Tien, J. W. and Kino, G. S., The nature of machining damage in brittle materials. *Proc. Roy. Soc. Lond.*, 1983, **A 385**, 461–475.
4. Malkin, S. and Ritter, J. E., Grinding mechanisms and strength degredation for ceramics. *Key Eng. Mater.*, 1992, **71**, 195–212.
5. Rice, R. W., Pohanka, R. C. and McDonough, W. J., Effect of stresses from thermal expansion anisotropy, phase transformations, and second phases on the strength of ceramics. *J. Am. Ceram. Soc.*, 1980, **63**(11-12), 703–710.
6. Rice, R. W., Machining of ceramics. In *Ceramics for High Performance Applications, Proc. of 2nd Army Mat. Tech.*, ed. J. J. Burke, A. E. Gorum and R. N. Katz. Metals and Ceramic Info. Center, Columbus, OH, 1974, pp. 287–343.
7. Rice, R. W., The effect of grinding direction on the strength of ceramics. In *The Science of Ceramic Machining and Surface Finishing, NBS Special Pub. 348*, ed. S. J. Schneider and R. W. Rice. US Govt. Printing Office, Washington, DC, 1972, pp. 365–376.
8. Mecholsky, J. J., Freiman, S. W. and Rice, R. W., Effect of flaw geometry and fracture of glass. *J. Am. Ceram. Soc.*, 1977, **60**(3-4), 114–117.
9. Rice, R. W., Processing induced sources of mechanical failure in ceramics. In *Processing of Crystalline Ceramics*, ed. H. Palmour III, R. F. Davis and T. M. Hare. Plenum Publishing Corp, New York, 1978, pp. 303–319.
10. Rice, R. W. and Mecholsky, J. J., The nature of strength controlling machining flaws in ceramics. In *The Science of Ceramic Machining and Surface Finishing II*, ed. B. J. Hockey and R. W. Rice. US Govt. Printing Office, Washington, DC, 1979, pp. 351–378.

11. Rice, R. W. Machining flaws and the strength-grain size behavior of ceramics. In *The Science of Ceramic Machining and Surface Finishing II*, ed. B. J. Hockey and R. W. Rice. NBS Special Pub. 562, pp. 429–454, 1979.
12. Rice, R. W., Mecholsky, J. J. and Becher, P. F., The effect of grinding direction on flaw character and strength of single crystal and polycrystalline ceramics. *J. Mater. Sci.*, 1981, **16**, 853–862.
13. R. W. Rice, Ceramic fracture features, observations, mechanisms, and uses. In *Fractography of Ceramic and Metal Failures*, ed. J. J. Mecholsky, Jr. and S. R. Powell, Jr. ASTM, STP 827, 1984, pp. 5–103.
14. Rice, R. W., Perspective on fractography. In *Adv. Cer., 22, Fractography of Glasses and Ceramics*, ed. V. D. Frechette and J. R. Varner. Am. Cer. Soc, Westerville, OH, 1988, pp. 3–56.
15. Rice, R. W., Effects of ceramic microstructural character on machining direction- strength anisotropy. In *Machining of Advanced Materials, NIST Special Pub. 847*, ed. S. Jahanmir. US Govt. Printing Office, Washington, DC, 1993, pp. 185–204.
16. Rice, R. W., Correlation of machining- grain- size effects on tensile strength with tensile strength- grain-size behavior. *J. Am. Ceram. Soc.*, 1993, **76**(4), 1068–1070.
17. Rice, R. W., Porosity effects on machining direction-strength anisotropy and failure mechanisms. *J. Am. Ceram. Soc.*, 1994, **77**(8), 2232–2236.
18. Rice, R. W., *Porosity of Ceramics*. Marcel Dekker, New York, 1998.
19. Rice, R. W., *Mechanical Properties of Ceramics and Composites: Grain and Particle Effects*. Marcel Dekker, New York, 1999.
20. Busch, D. M. and Prins, J. F., A basic study of the diamond grinding of alumina. In *The Science of Ceramic Machining and Surface Finishing, NBS Special Pub. 348*, ed. S. J. Schneider and R. W. Rice. US Govt. Printing Office, Washington, DC, 1972, pp. 73–87.
21. Lewis, D., Huyn, T. C. and Reed, J. S., Processing defects in partially stabilized zirconia. *Am. Ceram. Soc. Bull.*, 1980, **59**(2), 244–245.
22. Pujari, V., Tracey, D. M., Foley, M. R., Paille, N. I., Pelletier, P. J., Sales, L. C., Wilkens, C. A. and Yeckley, R.L., *Development of Improved Processing and Evaluation Methods for High Reliability Structural Ceramics for Advanced Heat Engine Applications, Phase I*. Norton Co. Advanced Ceramics Final Report for US Dept. Energy contract DE-AC05-84OR21400, 9/1993.
23. Pujari, V. K., Tracey, D. M., Foley, M. R., Paille, N. I., Pelletier, P. J., Sales, L. C., Wilkens, C. A. and Yeckley, R. L., Reliable ceramics for advanced heat engines. *Am. Ceram. Soc. Bull.*, 1995, **74**(4), 86–90.
24. Quinn, G. D., Fractographic analysis of machining cracks in silicon nitride rods and bars. In *Fractography of Glasses and Ceramics IV*, ed. J. Varner and G. Quinn. American Ceramic Soc, Westerville, OH, 2001.
25. Rice, R. W., Review, ceramic tensile strength: grain size relations: grain sizes, slopes, and branch intersections. *J. Mater. Sci.*, 1997, **32**, 1673–1692.
26. Rice, R. W. and Speronello, B. K., Effect of microstructure on rate of machining of ceramics. *J. Am. Ceram. Soc.*, 1976, **59**(7-8), 330–333.
27. Munro, R. G. and Freiman, S. W., Correlation of fracture toughness and strength. *J. Am. Ceram. Soc.*, 1999, **82**(8), 2246–2248.
28. Rice, R. W., Relation of tensile strength-porosity effects in ceramics to porosity dependence of Young's modulus and fracture energy, porosity character and grain size. *Mater. Sci. Eng.*, 1989, **A112**, 215–224.
29. Singh, J. P., Kirkar, A. V., Shetty, D. K. and Gordon, R. S., Strength-grain size relations in polycrystalline ceramics. *J. Am. Ceram. Soc.*, 1979, **62**(3-4), 179–182.
30. Evans, A. G., A dimensional analysis of the grain-size dependence of strength. *J. Am. Ceram. Soc.*, 1980, **63**(1-2), 115–116.
31. Virkar, A. V., Shetty, D. K. and Evans, A. G., Grain-size dependence of strength. *J. Am. Ceram. Soc.*, 1981, **64**(1), 56–57.
32. Wu, C. Cm. and McKinney, K. R., The effect of surface finishing on the strength of commercial hot pressed Si_3N_4. In *The Science of Ceramic Machining and Surface Finishing II*, ed. B. J. Hockey and R. W. Rice. US Govt. Printing Office, Washington, DC, 1979, pp. 477–481.
33. Anderson, C. A. and Bratton, R. J., Effect of surface finish on the strength of hot pressed silicon nitride. In *The Science of Ceramic Machining and Surface Finishing II*, ed. B. J. Hockey and R. W. Rice. US Govt. Printing Office, Washington, DC, 1979, pp. 463–474.
34. Ota, M. and Miyahara, K., *The Influence of Grinding on the Flexural Strength of Ceramics*. Soc. Manufacturing Engineers Tech. Paper MR90-538, 1990.
35. Mayer, J. E. and Fang, G. P., Diamond grinding of silicon nitride ceramic. In *Machining of Advanced Materials, NIST Special Pub. 847*, ed. S. Jahanmir. US Govt. Printing Office, Washington, DC, 1993, pp. 205–222.
36. Kishi, K., Umebavashi, S., Tani, E., Shobu, K. and Cho, D.-H., Room-temperature strength of mirror-ground β-sialon ($z=0.5$) fabricated from Si_3N_4 and aliminum iso-propoxide. *J. Mater. Sci. Lett.*, 1999, **18**, 1013–1014.
37. Cranmer, D. C., Tressler, R. E. and Bradt, R. C., Surface finish effects and the strength-grain size relation in SiC. *J. Am. Ceram. Soc.*, 1977, **60**(5-6), 230–237.
38. Bradt, R. C., Dulberg, J. L. and Tressler, R. E., Surface finish effects and the strength-grain size relationship in MgO. *Acta Metall.*, 1976, **24**, 529–534.
39. Tressler, R. E., Langensiepen, R. A. and Bradt, R. C., Surface-finish effects on strength-vs-grain-size relations in polycrystalline Al_2O_3. *J. Am. Ceram. Soc.*, 1974, **57**(5), 226–227.
40. McKinney, K. R. and Herbert, C. M., Effect of surface finish on structural ceramic failure. *J. Am. Ceram. Soc.*, 1970, **53**(9), 513–516.
41. Gupta, T. K., Strengthening by surface damage in metastable tetragonal zirconia. *J. Am. Ceram. Soc.*, 1980, **63**(1-2), 117.
42. Hanney M. J. and Morrell, R., Factors influencing the strength of a 95% alumina ceramic: In *Proc. Brit. Cer. Soc. 32 Engineering with Ceramics*, ed. R. W. Davidge. 1982, pp. 277–290.
43. Hockey, B. J., Observations on mechanically abraded aluminum oxide crystals by transmission electron microscopy. In *The Science of Ceramic Machining and Surface Finishing, NBS Special Pub. 348*, ed. S. J. Schneider and R. W. Rice. U. S. Govt. Printing Office, Washington, DC, 1972, pp. 333–339.
44. Stokes, R. J., Effects of surface finishing on mechanical and other physical properties of ceramics. ibid, 1972, pp. 343–352.
45. Johnson-Walls, D., Evans, A. G., Marshall, D. B. and James, M. R., Residual stresses in machined ceramic surfaces. *J. Am. Ceram. Soc.*, 1986, **69**(1), 44–47.
46. Samuel, R., Chandraekar, S., Farris, T. N. and Licht, R. H., Effect of residual stresses on the fracture of ground ceramics. *J. Am. Ceram. Soc.*, 1989, **72**(10), 1960–1966.
47. Ahn, Y., Chandraseker, S. and Farris, T. N., Measurement of residual stresses in machined ceramics using the indentation technique. In *Machining of Advanced Materials, NIST Special Pub. 847*, ed. S. Jahanmir. US Govt. Printing Office, Washington, DC, 1993, pp. 135–146.
48. Pfeiffer, W. and Hollstein, T. Damage determination and strength prediction of machined ceramics by X-ray diffraction techniques. ibid, 1993, pp. 235–245.
49. Kirchner, H. P. and Isaacson, E. D., Residual stresses in hot-pressed Si_3N_4 grooved by single-point grinding. *J. Am. Ceram. Soc.*, 1982, **65**(1), 55–60.

50. Chou, I. A., Chan, H. M. and Harmer, M. P., Machining-induced surface residual stress behavior in Al_2O_3–SiC nano-composites. *J. Am. Ceram. Soc.*, 1996, **79**(9), 2403–2409.
51. Reed, J. S. and Lejus, A.-M., Affect of grinding and polishing on near-surface phase transformation in zirconia. *Mater. Res. Bull.*, 1977, **12**, 949–954.
52. Wahi, R. P. and Ilschner, B., Fracture behavior of composites based on Al_2O_3–TiC. *J. Mater. Sci.*, 1980, **15**, 875–885.
54. Rice, R. W., Toughening in ceramic particulate and whisker composites. *Ceram. Eng. Sci. Proc.*, 1990, **11**(7-8), 667–694.
55. Binns, D. B., Some properties of two-phase crystal-glass solids. In *Science of Ceramics, Vol. 1*, ed. G. H. Stewart. Academic Press, New York, 1962, pp. 315–334.
56. Pezzotti, G. and Nishida, T., Effect of size and morphology of particulate SiC dispersions on fracture behavior of Si_3N_4 without sintering aids. *J. Mater. Sci.*, 1994, **29**, 1765–1772.
57. Endo, H., Ueki, M. and Kubo, H., Microstructure and mechanical properties of hot pressed SiC–TiC composites. *J. Mater. Sci.*, 1991, **26**, 3769–3774.
58. Rice, R. W., Wu, C.Cm. and Borchelt, F., Hardness-grain-size relations in ceramics. *J. Am. Ceram. Soc.*, 1994, **77**(10), 2539–2553.
59. Rice, R. W., Freiman, S. W. and Mecholsky, J. J., The dependence of strength-controlling fracture energy on the flaw-size to grain-size ratio. *J. Am. Ceram. Soc.*, 1980, **63**(3-4), 129–136.